[15]J. Wilks, *The Properties of Liquid and Solid Helium* (Oxford U. P., London, 1967), p. 677, Table A14.

[16]Note that this differs significantly from the simple interpolation formula used by De Bruyn Ouboter *et al.*, in Ref. 1.

[17]R. Radebaugh, Natl. Bur. Std. (U. S.) Technical Note No. 362 (U. S. GPO, Washington, D. C., 1967).

[18]The value of m_4^* is, however, very sensitive to the way in which the theory is fitted to the data. For example, the best fit to the six lowest-temperature points in Fig. 2 gives $\epsilon_{40} = -6.67$ K and $m_4^* \approx 3.7\, m_4$.

[19]De Bruyn Ouboter *et al.* (Ref. 1) found $\epsilon_{40} = -6.45$ K, and Edwards and Daunt (Ref. 3) found $m_4^* = 5.3\, m_4$.

PHYSICAL REVIEW A VOLUME 4, NUMBER 3 SEPTEMBER 1971

Relaxation Oscillations in Stimulated Raman and Brillouin Scattering*

R. V. Johnson and J. H. Marburger
University of Southern California, Los Angeles, California 90007
(Received 21 December 1970)

The equations describing the transfer of intensity from a pump beam *simultaneously* to forward and backward stimulated scattered beams in an infinite medium are shown to lead to pulsations similar to relaxation oscillations in the scattered intensities. The period of the pulsations is simply related to the gain length for the forward-scattered beam, and may be much longer than the ordinary transient time (related to the damping of material excitations) usually associated with stimulated scattering. Similar oscillations occur for backward scattering alone (stimulated Brillouin scattering) if the scattering medium is finite. In this case the period equals the photon round-trip time in the medium if the latter exceeds the backward gain length. Both phenomena should be observable in scattering from gases such as N_2 and H_2 at high pressure, and may also play a role in determining the temporal structure of light scattered from the region of a self-focus in liquids.

I. INTRODUCTION

The transient growth of light scattered inelastically from thermal or quantum fluctuations in a medium has been examined theoretically by previous authors in a variety of special cases. A typical analysis begins with the set of coupled equations describing the motion of a limited number of modes of the optical radiation field and of the medium. These are then simplified using various plausible assumptions about the mechanisms responsible for the particular phenomenon under investigation. Thus Kroll[1] has analyzed the growth of stimulated Brillouin scattering in the low conversion regime where linearized equations are valid. Similar studies of stimulated Raman, thermal, and Rayleigh wing scattering have appeared more recently.[2] Tang[3] has extended the Brillouin scattering analysis to the nonlinear high conversion regime. Recently Maier, Kaiser, and Giordmaine[4] have investigated transient solutions of nonlinear equations describing the interaction of backward-Raman-scattered light with the driving beam. In this paper we report the results of a similar theoretical study in which it was found that the backward-scattered beam experiences transient behavior resembling relaxation oscillations, the duration of which may vastly exceed the transient periods studied in the linear regime. This behavior has nothing to do with self-focusing, but occurs under very general conditions.

There are two related kinds of "relaxation" oscillations in stimulated scattering situations involving backward-scattered waves. Both are most conveniently observed in the time dependence of the backscattered intensity at the entrance to the scattering medium.

The simplest case is the *finite-cell oscillation* which can occur whenever a forward-traveling pump beam drives a stimulated scattered beam in the backward direction in a finite medium. The period is proportional to the sample length L, and therefore no oscillations of this type are observed if the sample length is infinite.

In contrast, *three-wave oscillations* may be observed even in a medium of infinite length, but stimulated scattering must occur in the forward as well as in the backward direction. These are similar to the finite-cell oscillations in that the depletion of the incident pump beam intensity by the forward wave effectively truncates the region in which the backward wave experiences gain. Thus the period is proportional to the distance L_f over which the forward wave travels before growing to an appreciable fraction of the pump intensity. (We are assuming for simplicity that the pump intensity remains constant at the cell entrance, after the

beam is switched on abruptly.) In either case the oscillations may occur for many cycles before the intensities relax to a steady state.

In Sec. II we discuss the equations from which this behavior is inferred, and how they are related to realistic experimental cases. Section III contains a detailed account of the properties of the solutions of these equations, and Sec. IV a numerical example for hydrogen and nitrogen gas.

II. APPROXIMATE EQUATIONS DESCRIBING STIMULATED SCATTERING

We restrict ourselves from the beginning to the one-dimensional geometry in which light may travel either forward ($+z$ direction) or backward. Furthermore, we examine only a single mode of the scattered light at each of the widely spaced frequencies of interest, or at most a group of modes of the same polarization whose frequencies lie in narrow intervals about a given value. We also ignore the effects of optical dispersion, an omission that will be corrected in future publications dealing with more specific experiments.

Our hypothetical system consists of a medium occupying the "cell" $0<z<L$ and a monochromatic "pump" beam initially of intensity I_0 traveling in the $+z$ direction which first enters the medium at $t=0$. Subsequently one observes forward- and backward-traveling waves at new frequencies, the most intense of which are usually Raman and Brillouin Stokes waves. These waves arise from inelastic stimulated scattering processes during which vibrational excitations are created within the medium. The corresponding scattering rates are vanishingly small just after the pump beam strikes the medium, but increase to their full values within a certain transient period. During this period, the vibrations of the medium from which the scattering takes place have not yet been driven to their steady-state values in the presence of the pump beam (which is usually not significantly depleted during this short time).

In this paper we shall be interested in time-dependent phenomena of much longer duration than this transient time. We therefore assume that the material oscillations reach their steady states instantly. In this case it is well known that one may "adiabatically eliminate" the equations for the material displacements and work only with equations describing the amplitudes of the interacting modes of the radiation field. There are several ways of deriving the final equations: Tang has done it for Brillouin scattering[3] and Maier *et al.* for Raman scattering.[4] The result, when both are considered simultaneously, is

$$\frac{\partial I}{\partial z}+\frac{1}{v}\frac{\partial I}{\partial t}=-gI(F+B+2a)-g'I(B'+a'), \quad (1)$$

$$\frac{\partial F}{\partial z}+\frac{1}{v}\frac{\partial F}{\partial t}=gI(F+a), \quad (2)$$

$$\frac{\partial B}{\partial z}-\frac{1}{v}\frac{\partial B}{\partial t}=-gI(B+a), \quad (3)$$

$$\frac{\partial B'}{\partial z}-\frac{1}{v}\frac{\partial B'}{\partial t}=-g'I(B'+a'). \quad (4)$$

Here I, F, B, and B' are the intensities of the pump, forward Raman, backward Raman, and backward Brillouin beams, respectively; $v=c/n$ is the velocity of light in the medium, assumed the same for all the waves; g and a are the spatial gain coefficient and "noise" intensity for the Raman process; and g' and a' are the corresponding quantities for Brillouin scattering. The noise terms may be removed from the equations by the change of variable $\overline{F}\equiv F+a$, etc. Expressions for g and g' are given by Hagenlocker *et al.* [Eqs. (7) and (5) of Ref. 5] in a convenient form.

If g and g' are equal, Eqs. (1)–(4) can be reduced to three equations in I, F, and $B+B'$ which have the same form as the equations describing Raman scattering alone. But even if g and g' are unequal, three equations may suffice to give an adequate description of the dynamics of the system. To see this, the reader may integrate (3) and (4) along the common characteristic $x=\frac{1}{2}(vt+z)$ from a point y_0 at which $B=B'=0$. One finds

$$\overline{B}'/a'=(\overline{B}/a)^{g'/g}. \quad (5)$$

Thus, if a and a' are comparable, and $g'>g$, B may be ignored in the stimulated scattering regime $B\gg a$. More generally, of two modes sharing the same characteristic, that with the larger gain will dominate. For this reason, most of our analysis deals with the solutions of the three-wave system

$$\frac{\partial I}{\partial x}=-gI(F+a)-g'I(B'+a'), \quad (6)$$

$$\frac{\partial F}{\partial x}=gI(F+a), \quad (7)$$

$$\frac{\partial B'}{\partial y}=g'I(B'+a'), \quad (8)$$

where $x=\frac{1}{2}(z+vt)$, $y=\frac{1}{2}(vt-z)$, and the primed quantities refer to the backward wave with the larger gain.

If the backward scattering is overwhelmingly larger than the forward, $g'\gg g$, the situation may be represented adequately by the system

$$\frac{\partial I}{\partial x}=-g'I(B'+a'), \quad (9)$$

$$\frac{\partial B'}{\partial y}=g'I(B'+a'). \quad (10)$$

All three systems (1)–(4), (6)–(8), and (9) and (10) display relaxation oscillations if the scattering is

driven by a pump pulse longer than the period of the oscillation, and if the medium is long enough. Only finite-cell oscillations occur for the system (9), (10).

III. PROPERTIES OF RELAXATION OSCILLATIONS

A. Finite-Cell Oscillations

It is best to begin with the simplest system (9), (10) in which the backward wave B' is initially zero within the cell $0 \le z \le L$. Solutions are most easily obtained when L is infinite. Using the technique described by Maier *et al.*,[4] one finds the solutions

$$I(z,t) = D^{-1} e^{-g a' z} \times \{ I_0 \exp[-\tfrac{1}{2} g'(I_0 + a')(vt - z)] + a' \} \theta(vt - z) \quad (11)$$

and

$$B'(z,t) + a' = a' D^{-1} (I_0 + a') \theta(vt - z) \ , \quad (12)$$

where

$$D \equiv I_0 + a' - I_0 e^{-g' a' z} \{ 1 - \exp[-\tfrac{1}{2} g'(I_0 + a')(vt - z)] \} \ . \quad (13)$$

The pump pulse at $z = 0$ is $I(0,t) = I_0 \theta(t)$, where $\theta(t) = 1$ for $t > 0$ and zero otherwise. Evaluating B' at $z = 0$, we find the monotonically increasing function

$$B'(0,t) + a' = \frac{a'(I_0 + a')}{a' + I_0 \exp[-\tfrac{1}{2} g'(I_0 + a') vt]} \ , \quad (14)$$

which tends asymptotically to $B'(0, \infty) = I_0$.

The corresponding solutions for a finite cell may also be obtained analytically, but with much greater effort. Clearly the solution (14) must be correct for $t \le 2L/v$, the earliest time at which information about the termination of the medium can reach $z = 0$. During the next intervals $2nL/v \le t \le 2(n+1)L/v$, $n = 1, 2, 3, \ldots$, the solution has a form depending upon n which becomes more complicated as n increases. The solution and its derivation for $n \ge 1$ are given in the Appendix. Figure 1 shows $B'(0,t)$ for a variety of cell lengths. In each case the oscillations have period $2L/v$ and tend toward the steady-state value indicated. This steady-state value can be obtained from Eqs. (9) and (10) by seeking time-independent solutions $I(z)$ and $B'(z)$ satisfying $I(0) = I_0$ and $B'(L) = 0$. The result for $0 \le z \le L$ is

$$B'(z) + a' = \frac{[B'(0) + a'][I_0 - B'(0) - a']}{I_0 \exp[I_0 - B'(0) - a'] g' z - B'(0) - a'} \ , \quad (15)$$

where $B'(0)$, evaluated from this expression, is plotted in Fig. 2. In this figure the cell length is measured in units $L_b \equiv (1/g'I_0) \ln(I_0/a')$. The curves $B'(0)$ vs $L^* \equiv L/L_b$ for different values of I_0/a are all nearly alike, suggesting that $B'(0)$ is to a good approximation a function of L^* alone. The significance of L_b is that for a cell of this length the backward intensity at $z = 0$ is $\frac{1}{2} I_0$ after one round-trip time. For an infinite cell, $B'(0) = B'(0, \infty) = I_0$ from (14).

An intuitive understanding of the oscillations may be obtained by examining Figs. 3 and 4. Figure 3 shows a coarse "movie" of $B'(z,t)$ and $I(z,t)$ for an infinite medium. Notice that the forward-traveling laser pulse near the leading edge has length, by (11),

$$L_p \approx (2/g'I_0) \ln(I_0/a') \quad (I_0 \gg a) \ . \quad (16)$$

A portion of the backward-traveling signal which begins at the forward pulse front grows nearly exponentially throughout L_p, during which it is exposed to nearly the full incident intensity I_0. After passing through this region it has grown to somewhat less than $a' \exp(\frac{1}{2} g' I_0 L_p)$. During the remainder of its journey back to $z = 0$, it sees a heavily depleted pump beam and therefore grows correspondingly more slowly. The z dependence is actually hyperbolic in this region rather than expo-

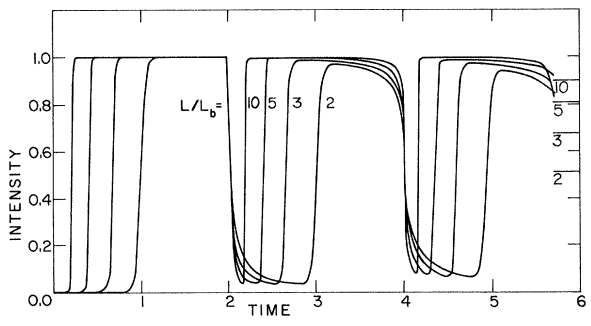

FIG. 1. Two-wave finite-cell oscillations in backward stimulated Brillouin scattering for various cell lengths. Ordinate shows intensity B' at cell entrance in units of incident pump intensity $I_0 = 10^{16} a'$. Time is measured along abscissa in units L_b/v. Steady-state values of B' are indicated at the right edge. Incident pump intensity at cell entrance is constant for positive times, zero otherwise.

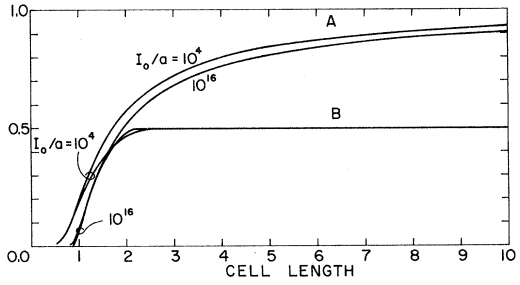

FIG. 2. Steady-state values of the backward-scattered intensity for stimulated Brillouin (A) and Raman (B) scattering from finite cells, measured at the cell entrance. Abscissa is cell length in units L_b. Ordinate as in Fig. 1. The curves are relatively insensitive to the value of I_0/a, which is indicated for the largest and smallest values investigated.

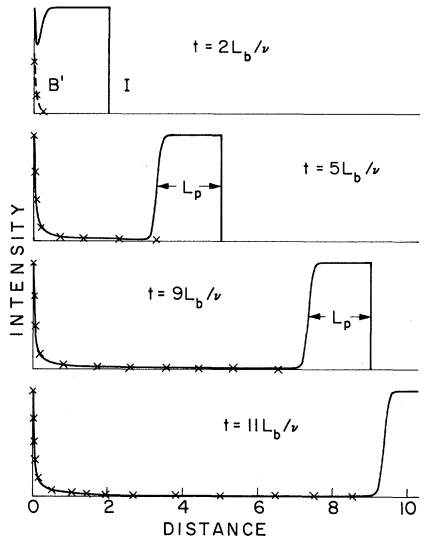

FIG. 3. "Movie" of the pump (——) and backward stimulated Brillouin Stokes intensity (x---x). Distance is measured in units L_b. The pulse length L_p is given initially by Eq. (16), but decreases eventually to zero as it propagates. Incident pump pulse is as in Fig. 1. $I_0 = 10^{16}a'$.

nential, as can be seen by expanding (12) for large t and small z, assuming $I_0/a' \gg 1$.

Turning now to Fig. 4, which shows the finite-cell case, one finds that after $t = L/v$, the maximum length of undepleted pump seen by a portion of the backward signal diminishes from L_p to zero. Consequently a backward-traveling noise signal cannot grow to a value in this region great enough to become appreciably augmented in the subsequent low-gain region. The result is a dramatic reduction of $B'(0, t)$ after $t = 2L/v$. When the backward intensity has decreased to a small value, which it does quite rapidly when $I_0 \gg a'$, the incident pump beam can pass well beyond the input face before becoming depleted again. This resembles the initial state of affairs, and the process repeats periodically with decreasing modulation depth until the steady state is achieved.

It is perhaps worth mentioning that similar oscillations do not occur with only a forward-traveling scattered wave. In this case the equations analogous to (9) and (10) are

$$\frac{\partial I}{\partial x} = -gI(F + a) \ , \tag{17}$$

$$\frac{\partial F}{\partial x} = gI(F + a) \ . \tag{18}$$

Choosing the same boundary conditions as before, we find

$$I(z, t) = I_0 \Delta^{-1}(I_0 + a) e^{-gz(I_0 + a)} \theta(vt - z) \ , \tag{19}$$

$$F(z, t) + a = a \, \Delta^{-1} (I_0 + a) \ , \tag{20}$$

where

$$\Delta \equiv a + I_0 e^{-gz(I_0 + a)} \ .$$

This solution is correct for a cell of any length, for $z \leq L$. Notice that F increases to $\frac{1}{2}I_0$ in the length

$$L_f = (1/gI_0) \ln(I_0/a) \quad \text{for } I_0/a \gg 1 \ . \tag{21}$$

The existence of unusual time dependence in a backward stimulated wave was first established by Maier, Kaiser, and Giordmaine[4] in connection with self-focusing. They used solutions of Eqs. (9) and (10) to analyze their results, but chose different boundary conditions. In particular, they assumed that the backward Stokes signal is initiated at $z = L$ by an external mechanism (self-focusing), whereupon it passes through a long region of undepleted pump beam from which it can extract energy. Consequently it is possible for the backward intensity to exceed I_0. In contrast, we allow the backward signal to begin growing as soon as the pump beam enters the medium at $z = 0$. In the absence of any additional enhancement of B' or I through focusing or self-focusing, this prevents the generation of sharp backward pulses of intensity greater than I_0 such as those studied by Maier *et al.*

Finally, we should point out that the entire analysis above (for the backward-wave problem) may be applied to the dispersive case in which the scattered wave propagates with velocity v'. One need only replace x by $\xi \equiv (v't + z)v/(v' + v)$ and y by $\eta \equiv (z - vt)v'/(v' + v)$. The equations in x and y retain their form, the only change in the problem being that the forward and backward characteristics are no longer perpendicular.

B. Three-Wave Oscillations

If forward as well as backward stimulated scat-

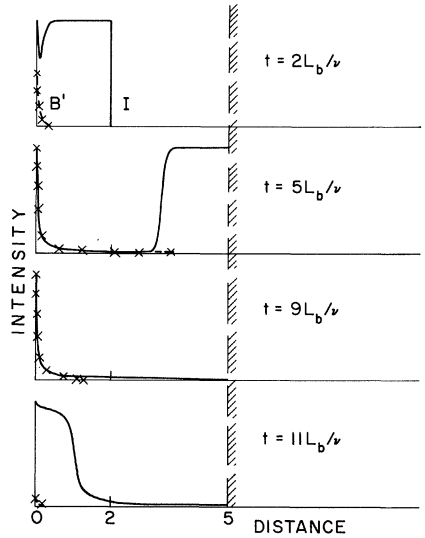

FIG. 4. Same as Fig. 3, but for a cell length of $5L_b$.

tering occurs, we may still have oscillations of period $2L/v$, but superimposed on these will be oscillations caused by the effective truncation of the medium by pump depletion to the forward-scattered waves. Unfortunately even for the simplest three-wave case represented by Eqs. (6)–(8) we have been unable to find analytic solutions except for the steady-state intensities. Nevertheless, the important features of the oscillations can be obtained by analogy with the two-wave finite-cell case. Finer details were obtained by numerical solution of the full set of equations.

We expect the backward-traveling signal to have little effect on the pump intensity just behind its forward-traveling leading edge. But the forward-scattered intensity F is maximum at this point at any instant and depletes the pump appreciably after traveling to about $z = L_f$, Eq. (21). We therefore expect the backward intensity B' to behave as if the medium were only of length $L = L_f$; that is, $B'(0, t)$ should exhibit oscillations of period $\sim 2L_f/v$. This is fully verified by numerical solutions of Eqs. (6)–(8), some of which are plotted in Figs. 5 and 6. The anticipated dependence of the period on g, I_0, and a have all been verified quite accurately using the numerical solutions.

Figures 5 and 6, and the explanation we have given, are for a very long cell. If the cell length is less then L_f, the forward beam cannot appreciably deplete the pump, and no pronounced three-wave oscillations will occur. If the cell is very long, oscillations occur as long as the forward gain is not greater than the backward gain: $g' \geq g$. If $g > g'$, then the pump will be spent before the backward wave can grow significantly. When $g < g'$, the

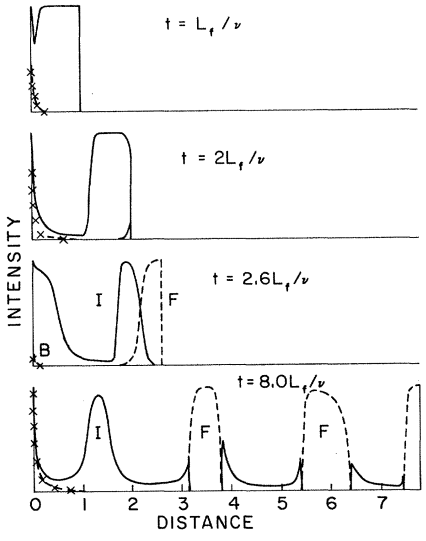

FIG. 5. Same as Fig. 3, but for stimulated Raman scattering. The forward and backward gains are equal in the case shown.

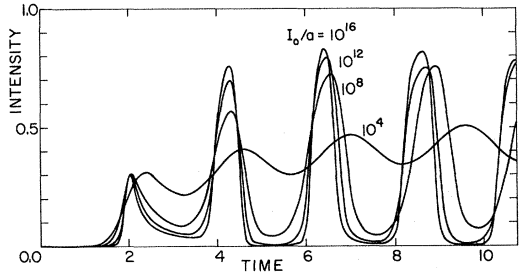

FIG. 6. Three-wave oscillations in backward stimulated Raman scattering for various ratios of the incident pump intensity to the noise level. Backward and forward gains are equal. Time is measured in units L_f/v.

maxima in $B'(0, t)$ have width roughly $\Delta t = 2(L_b - L)/v$ for the two-wave finite-cell case of Sec. III A. In that case the period and pulsation length are fixed by the cell length, but here the effective cell length for the backward wave increases as, on consecutive oscillations, the pump fails to recover completely to its previous value, thus decreasing the net forward gain. All these assertions, which are based upon our experience with the two-wave case, are verified by the numerical solutions.

Oscillations do not occur for very small incident intensities because the growth and decay processes are not sufficiently abrupt. We found numerically that I_0 must exceed a by somewhat less than 10^4 before well-defined oscillations appear.

Several numerical solutions were obtained for a pulsed incident beam whose time profile is Gaussian. As long as the pulse length exceeded the expected period at the peak intensity and the pulse peak was sufficiently strong ($\gtrsim 10^4 a$), the solutions showed oscillatory behavior. An exhaustive study of the influence of pulse shape on this structure has not yet been undertaken.

The time required for these oscillations to die is difficult to estimate. The accuracy of our numerical solutions cannot be trusted after very long times, and we can only report the following results: (a) The oscillations persist longest for $g \approx g'$; (b) for $I_0 = 10^{16} a$, $g' \approx 5g$ the intensities at the first and second minima in $B'(0, t)$ were $0.15 I_0$ and $0.55 I_0$, respectively; and (c) for $g = g'$, $I_0 = 10^4 a$, 16 maxima were observed in our longest computer run. The modulation depth was about 25% and the oscillations, centered on the steady-state value $B(0, \infty) = \frac{1}{2} I_0$, were nearly sinusoidal, showing no signs of decaying at this point.

The ultimate steady-state intensities may be obtained easily only for special values of the forward-to-backward-gain ratio g/g'. However, certain relations among the steady-state values can be obtained in the general case. The reader may easily verify that the functions

$$I + F - B \qquad (22)$$

and

$$(\bar{F})^{1/g}(\bar{B}')^{1/g'} \tag{23}$$

are integrals of the system (6)–(8) if the time dependence is removed. Thus, in the steady state,

$$I(L) = I_0 - B'(0) - F(L) \tag{24}$$

and

$$\bar{F}(L) = a[\bar{B}'(0)/a']^{g/g'} . \tag{25}$$

For equal gains these imply $B'(0) \leq \frac{1}{2}I_0$, the equality holding for infinite cell length. The precise value of $B'(0)$ must be obtained from a transcendental equation depending upon g/g'. For $g = g'$, $a = a'$, the dependence of $B'(0)$ on L and I_0/a is shown in Fig. 2. Here the cell length is measured in units L_f and the behavior of B' vs L/L_f is similar for a large range of incident intensities, as in the finite-cell case discussed in Sec. IIIA. When $L = \infty$, the pump beam is always depleted at infinity, and the steady values of B and F may be found by solving (24) and (25) simultaneously, setting $I(\infty) = 0$.

C. Influence of Additional Scattering Channels

When more than one forward and one backward stimulated scattering channel is available, we still expect to observe oscillations in the intensities of the scattered waves. In an infinite medium, the period is expected to be about $2L_f/v$, where L_f is the forward gain length (21) for the forward-scattering process with largest gain. With the addition of more scattering channels, the actual forward gain length in regions of relatively undepleted pump intensity will increase somewhat because of increased pump depletion. Figure 7 shows a typical numerical solution of Eqs. (1)–(4) which exhibits the expected oscillation. Also shown is the corresponding three-wave solution, which agrees well with the four-wave case as anticipated in Sec. II.

As before, we may obtain integrals of the system (1)–(4) for the steady-state behavior. The three "easy" integrals are

$$I + F - B - B' , \tag{26}$$

$$(\bar{B})^{1/g}/(\bar{B}')^{1/g'} , \tag{27}$$

$$(\bar{F}\bar{B})^{1/g} . \tag{28}$$

The fourth integral requires solution of an ordinary differential equation which the reader may easily derive. When $L = \infty$, the condition $I(\infty) = 0$ may be used together with (26)–(28) and $I(0) = I_0$ to find $F(\infty)$, $B(0)$, and $B'(0)$.

IV. STIMULATED SCATTERING IN GASES

While it is possible that transient pulsations of the type considered here may occur in stimulated scattering from liquids or solids, the analysis for these media is usually obscured by focusing or self-focusing effects. Thus, for a clear verification of the features we have described above, it seems desirable to investigate the time dependence of stimulated scattering in gases using unfocused pump beams. Such scattering has been observed, and with a suitable choice of gas and pressure, one can cause either stimulated Raman or stimulated Brillouin scattering to dominate.[5]

A complicating feature in gases is the possibility of rather long vibrational lifetimes, which could lead to an interference of the transient effects associated with beam depletion with the ordinary transient behavior associated with finite phonon lifetimes. We have not yet completed investigation of this interference, but we should like to call attention to the fact that all previous studies of transient stimulated Raman scattering have omitted the effect of competition between forward- and backward-scattered waves.[6] In the high-beam depletion case, which we have studied here, this competition arises because both waves extract energy from the same pump beam. In the ordinary transient case, the pump beam is usually almost undepleted, but the forward- and backward-wave equations are still coupled through the equation of motion of the vibrational coordinate. Nevertheless, as in the case of three-wave relaxation oscillations described above, one does not expect a strong effect from the backward wave until the pump pulse length exceeds a certain characteristic gain length corresponding to L_p defined in (16).

Hagenlocker, Minck, and Rado[5] observed stimulated Brillouin scattering in N_2 gas at 300 °K and pressures up to about 10^3 atm. At a pressure of about 100 atm they inferred a gain coefficient g'

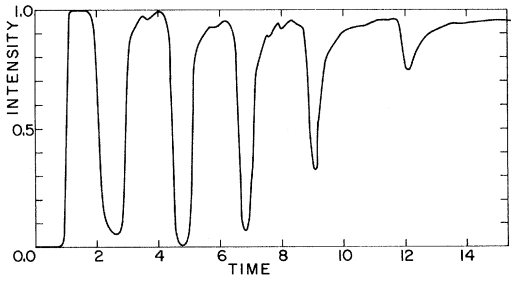

FIG. 7. Four-wave oscillations occurring when stimulated Raman and Brillouin scattering take place simultaneously. The Brillouin gain coefficient is twice that for the Raman process, and therefore the Brillouin-scattered intensity, which is shown here, far exceeds the Raman intensity. The backward intensity for the three-wave oscillation with backward-to-forward-gain ratio 2 follows a curve indistinguishable from that shown. Units are as in Fig. 6. Brillouin and Raman noise levels were assumed equal, but the curve is not very sensitive to deviations from this condition. The small-scale structure apparent near the maxima was probably introduced by our numerical-computation scheme.

of roughly 5×10^{-10} cm/w. Their data-reduction technique included transient effects, in what seems to be a reasonable way, for a pulse duration of 2×10^{-9} sec. This rather short interaction time was chosen to account for "an erratic spiking behavior" observed in the laser output. The origin of such spiking is now well understood and can be avoided by appropriate laser cavity design.[7] Thus pulses of a few times 10^{-8} sec duration can be obtained, and for these the effective Brillouin gain coefficient can exceed 10^{-8} cm/W for the case under consideration. Assuming a mean pulse power of about 30 MW in a cylindrical beam about 2 mm in diameter, and a noise intensity of about 10^{-5} W cm^2 sec, we find a critical length $L_p\approx7$ cm. To see finite-cell oscillations, the cell length must exceed L_p but still be much less than the incident pulse length, which is here greater than 3 m. Because the phenomenon is intensity dependent, one should examine only a portion of the scattered beam profile for oscillations.

The same authors,[5] and many others,[8] have also observed stimulated vibrational Raman scattering in H_2 gas under similar conditions. Here the gain does not appear to exceed about 10^{-9} cm/W, and L_p approaches 1 m for the laser parameters cited above. For observation of the three-wave oscillations one should use a cell as long as possible to avoid interference from the finite-cell effect. We are indebted to Professor Kaiser for the information that Maier has observed oscillations in the stimulated Raman scattering from H_2 gas which may have their origin in the mechanism described here. Whether the very complicated time dependence of the scattered light observed simultaneously with self-focusing in liquids can also be traced to this mechanism is an open question.

ACKNOWLEDGMENTS

This work was inspired by the note of Maier, Kaiser, and Giordmaine[4] which drew attention to the importance of backward-traveling waves in stimulated scattering. During our progress, we have benefited from the advice and assistance of many of our colleagues in the Quantum Electronics Group at the University of Southern California. Particularly helpful were Professor S. P. S. Porto and Professor W. G. Wagner.

APPENDIX: ANALYTICAL SOLUTIONS OF EQS. (9) AND (10) FOR $L<\infty$

Elementary manipulation of Eqs. (9) and (10) suffices to show that

$$gr(x)\equiv\frac{\partial}{\partial x}[\ln\overline{B}(x,y)]+g\overline{B}(x,y)$$

is independent of y. This equation is easily integrated for $1/\overline{B}$, the result being conveniently expressed in terms of

$$h(y)\equiv1/\overline{B}(x_0,y),\quad x_0=\text{const}$$

$$f(x)\equiv g\int_{x_0}^{x}dx'\exp\int_{x_0}^{x'}dx''\,gr(x'')\,.$$

With these definitions, we have

$$\overline{B}(x,y)=f'(x)/g[f(x)+h(y)]\,, \tag{A1}$$

$$I(x,y)=-h'(y)/g[f(x)+h(y)]\,, \tag{A2}$$

where a prime means differentiation with respect to the argument. The functions f and h satisfy equations which can be derived from (A1) and (A2) using the boundary conditions on $\overline{B}$ and I to be discussed below. Initial conditions for f and h, choosing $x_0=0$, are clearly $h(0)=1/a$ and $f(0)=0$.

We seek solutions for which $B=0$ on the cell exit face at $z=L$, or $\overline{B}(x,x-L)=a$. When $x\le L$ the forward pulse front, which enters the medium at $t=0$, has not yet reached the exit face. In this region we require that B vanish on the pulse front, or $\overline{B}(x,0)=a$ for $x\le L$. We refer to the region $0\le x\le L$ as region 0, and $\nu L\le x\le(\nu+1)L$, $\nu=1,2,\ldots$, as region ν. Functions whose domains are restricted to region ν will bear a Greek superscript: h^ν, f^ν. For simplicity we assume the simple step input pulse $I(y,y)=I_0\theta(y)$. Then for $x>0$, using (A1) and (A2), we find

$$dh^\nu(x)/dx=-gI_0[f^\nu(x)+h^\nu(x)],\qquad\nu=0,1,2,\ldots \tag{A3}$$

$$df^0(x)/dx=ga[f^0(x)+a^{-1}]\,, \tag{A4}$$

$$df^\nu(x)/dx=ga[f^\nu(x)+h^{\nu-1}(x-L)]\,,\qquad\nu=1,2,\ldots\,. \tag{A5}$$

These equations may be solved iteratively. To proceed, it is convenient to define the variable $u_\nu\equiv(x-\nu L)g(I_0+a)$ for x in region ν. Then (A3) and (A4) can be integrated to give

$$h^\nu(u_\nu)=e^{\delta u_\nu}[h^{\nu-1}(L')+\delta\int_0^{u_\nu}du'f^\nu(u')e^{-\delta u'}],\qquad\nu=1,2,\ldots$$

$$f^\nu(u_\nu)=e^{\epsilon u_\nu}[f^{\nu-1}(L')+\epsilon\int_0^{u_\nu}du'h^{\nu-1}(u')e^{-\epsilon u'}],\qquad\nu=1,2,\ldots$$

$$h^0(u_0)=a^{-1}(1+\delta e^{\epsilon u_0}-\delta e^{\delta u_0})\,,$$

$$f^0(u_0)=-a^{-1}(-e^{\epsilon u_0})\,,$$

where $\epsilon\equiv a/(I_0+a)$, $\delta\equiv\epsilon-1=-I_0(I_0+a)$, and $L'\equiv Lg(I_0+a)$. The reader can verify by induction that f^ν and h^ν may be written in the form

$$f^\nu(u)=-a^{-1}+\sum_{\mu=0}^{\nu}u^\mu(M_\mu^\nu e^{\epsilon u}+N_\mu^\nu e^{\delta u}),\quad u=u_\nu$$

$$h^\nu(u)=a^{-1}+\sum_{\mu=0}^{\nu}u^\mu(\overline{M}_\mu^{\,\nu}e^{\epsilon u}+\overline{N}_\mu^{\,\nu}e^{\delta u}),\qquad u=u_\nu$$

where the M's and N's satisfy

$$M_0^\nu = a^{-1} + f^{\nu-1}(L') + \epsilon \sum_{\mu=0}^{\nu-1} \bar{N}_\mu^{\nu-1} \mu! \ ,$$

$$M_\mu^\nu = \epsilon \bar{M}_{\mu-1}^{\nu-1}/\mu, \qquad 1 \le \mu \le \nu$$

$$N_\mu^\nu = -\epsilon \sum_{\lambda=\mu}^{\nu-1} \bar{N}_\lambda^{\nu-1} \lambda!/\mu!, \qquad 0 \le \mu \le \nu - 1$$

$$\bar{M}_\mu^\nu = \delta \sum_{\lambda=\mu}^{\nu} (-1)^{\mu-\lambda} M_\lambda^\nu \lambda!/\mu!, \quad 0 \le \mu \le \nu$$

$$\bar{N}_0^\nu = -a^{-1} + h^{\nu-1}(L') - \delta \sum_{\mu=0}^{\nu} (-1)^\mu M_\mu^\nu \mu! \ ,$$

$$\bar{N}_\mu^\nu = \delta N_{\mu-1}^\nu/\mu \ , \quad 1 \le \mu \le \nu \ .$$

We apologize for the opacity of this form. Nevertheless, it does allow more rapid calculation of numerical results than direct computer solution of the original set of equations. The final formulas for I and B may be written

$$I^\nu(x, y) = I_0 \theta(y)[f^\nu(y) + h^\nu(y)]/[f^\nu(x) + h^\nu(y)] \ ,$$

$$B^\nu(x, y) = a[h^{\nu-1}(x) - h^\nu(y)]/[f^\nu(x) + h^\nu(y)] \ .$$

*Work partially supported by the U. S. Army Research Office, Durham, under Grant No. DA-ARO-D-31-124-6920 and the Joint Services Electronics Program (U. S. Army, Navy, and Air Force), under Grant No. AF-AFOSR-69-1622A.

[1]N. M. Kroll, J. Appl. Phys. 36, 34 (1965).
[2]N. M. Kroll and P. L. Kelley (unpublished); C. S. Wang, Phys. Rev. 182, 482 (1969).
[3]C. L. Tang, J. Appl. Phys. 37, 2945 (1966).
[4]M. Maier, W. Kaiser, and J. A. Giordmaine, Phys. Rev. 177, 580 (1969); Phys. Rev. Letters 17, 1275 (1966).
[5]E. E. Hagenlocker, R. W. Minck, and W. G. Rado, Phys. Rev. 154, 226 (1967).
[6]See Wang, Ref. 2, and work cited therein.
[7]G. L. McAllister, M. M. Mann, and L. G. DeShazer, IEEE J. Quantum Electron. QE-6, 44 (1970).
[8]N. Bloembergen, G. Bret, P. Lallemand, A. Pine, and P. Simova, IEEE J. Quantum Electron. QE-3, 197 (1967).

PHYSICAL REVIEW A VOLUME 4, NUMBER 3 SEPTEMBER 1971

Filamentary Tracks Formed in Transparent Optical Glass by Laser Beam Self-Focusing. I. Experimental Investigation*

George N. Steinberg
Perkin-Elmer Corporation, Research Department, 50 *Danbury Road*, *Wilton, Connecticut* 06897
(Received 14 January 1971)

The permanent damage in optical glass investigated here is characterized by filamentary tracks of fine fractures. These tracks are a few micrometers in diameter, straight to within 0.7 μm, up to 9 cm long, and collinear with the incident laser beam. There may also be damage stars (regions of fracture gross compared with the track diameter). These damage stars are usually near the upstream ends of the tracks. Track formation is characterized by a flash of side-scattered white light from the track, laser light side-scattered from the damage stars, a marked increase in the exit divergence angle of the laser beam, and a weak back-scattered pulse of laser light. The back-scattered pulse preserves the polarization of the incident beam, is of shorter duration than the incident laser pulse, and has a frequency shift corresponding to Brillouin scattering from a free compressional sound wave in the glass. Track formation is accompanied by a detectable cylindrical sound wave. The track formation threshold is repeatable at different locations in the glass sample. Both the power threshold and the energy-density threshold are rapidly varying functions of the incident beam radius at focus. The threshold power is as low as 10 kW for a ruby-laser beam sharply focused in dense flint glass, and more than 2 MW for an unfocused beam in fused silica.

INTRODUCTION

The type of filamentary track formation in glass we investigated was first reported by Hercher.[1] The experiments we performed established the threshold dependence on beam size for three types of optical quality nonabsorbing glass. We found the threshold was repeatable in different glass samples of the same type, given the same incident beam conditions. We also investigated the characteristics of the many emissions accompanying track formation, and attempted to account for all